24^{th} *Computer Vision Winter Workshop*
Friedrich Fraundorfer, Peter M. Roth, Fabian Schenk (eds.)
Stift Vorau, Austria, February 6–8, 2019
DOI: 10.3217/978-3-85125-652-9-05

Counting slope regions in the surface graphs

Darshan Batavia, Walter G. Kropatsch
PRIP Group 193/03
TU Wien, Austria
{darshan,krw}@prip.tuwien.ac.at

Rocio Gonzalez-Diaz, Rocio M. Casablanca
Applied Maths 1
University of Seville, Spain
{rogodi,rociomc}@us.es

Abstract. *The discrete version of a continuous surface sampled at optimum sampling rate can be well expressed in form of a neighborhood graph containing the critical points (maxima, minima, saddles) of the surface. Basic operations on the graph such as edge contraction and removal eliminate non-critical points and collapse plateau regions resulting in the formation of a graph pyramid. If the neighborhood graph is well-composed, faces in the graph pyramid are slope regions. In this paper we focus on the graph on the top of the pyramid which will contain critical points only, self-loops and multiple edges connecting the same vertices. We enumerate the different possible configurations of slope regions, forming a catalogue of different configurations when combining slope regions and studying the number of slope regions on the top.*

1. Introduction

There is a strong correlation between an image and a geographical surface. A digital image can be perceived as a geographical surface where the height of a point in the surface is directly proportional to the pixel intensity at that coordinate. The critical points: maxima, minima and saddle from the image correspond to the hills, dales and ridge in terrain. Configurations of critical points and slope lines of surfaces were discussed by Cayley [3] and Maxwell [17]. Their observations are with respect to the earth's topography but play a significant role in exploiting properties of smooth surfaces. Nackmann Lee [15] represented and studied their possible configurations in form of a graph for a Morse function of two variables (also called 2D Morse function).

Edelsbrunner *et al.* [8, 7] attempt to capture the topological aspect of the images by constructing a hierarchy of increasingly coarse Morse-Smale complexes and decompose a piecewise linear 2D-manifold. Degenerated critical points were excluded in that study. Categorization of critical points and slope points was simplified in [4] with the use of Local Binary Patterns (LBPs).

Cerman *et al.* [5] use LBP to orient the edges of the neighborhood graph of an image. By using contraction and removal operations on the edges of the neighborhood graph, they generate progressively smaller graphs. Stacking such smaller graphs forms a graph pyramid, used for multi-resolution image segmentation. A similar approach can be found in [19] which uses a super pixel hierarchy for the formation of the pyramid used for a similar purpose.

For a 1D Morse function, critical points x are identified if its first derivative is null. For a 2D Morse function, Critical points are determined by vanishing first derivatives. To classify the critical points in 2D we study the determinant of the Hessian matrix H. If it is non-zero, then the point is a non-degenerate critical point. Otherwise, it is a degenerate critical point which is excluded from a Morse function. The signs of the eigenvalues of H are used to classify the point in maximum, minimum or saddle points.

In [12, 11] the authors form a slope complex extending the model developed in [8, 7], to include degenerated critical points. In this paper, we allow the occurrence of degenerated critical points where either the Hessian matrix is nilpotent or semi-definite. If the Hessian matrix is nilpotent, the neighborhood of the point is a plateau region, which is a local surface patch of points with the same height. If the Hessian is a positive semi-definite matrix, then one of it's eigenvalue is zero and the neighborhood of the point contains a level curve inside a 2D surface.

In formation of the graph pyramid, the top level of the pyramid is expected to be preserve only with the critical points. Also there is no unique configura-

tion in which these critical points are connected. Euler's formula [6, theorem 4.2.7] provides the lower bound for the number of faces formed by connecting the vertices, provided the number of edges are known. It further get complicated when we allow the self-loops. In this paper, we study all the different configuration of faces also called as slope regions which are formed by connections of the critical vertices. We also present an approach to count the number of slope regions in a given primal graph which includes self-loops. In this paper we avoid use of derivatives and instead use Local Binary Patterns (LBPs) to determine the category of a point (minimum, maximum, saddle or slope) in discrete domain which is explained in Section 2 along with few other necessary definitions. Section 3 introduces the prototypes of slope regions with minimal number of edges. In Section 4 we summarize the effect of contracting the saddle components. Section 5 is dedicated to the combinations of slope regions which form the basis to represent a surface. We provide a formula to count the number of slope regions of a surface to ski down from its embedded graph in Section 6. We generalize the count made in [11] in the sense that in this paper the primal graph can contain self-loops. Finally, Section 7 is devoted to conclusions and future works. The appendix contains some examples of applying LBP pyramids on the digital images.

2. Basic definitions

A digital image P can be visually perceived as a sampled version of a geographical terrain model which is a continuous surface denoted by S. The sampling frequency to choose the samples should satisfy the Nyquist criterion with respect to the minimum distance between any two critical points. The digital image P can be efficiently represented by a dual pair of plane graphs. The primal graph or neighborhood graph $G = (V, E)$ is formed by vertices $v \in V$ corresponding to pixels $p \in P$ connected to the four adjacent neighbors by edges $e \in E$. The dual of the primal graph is the graph $\overline{G} = (\overline{V}, \overline{E})$ where every dual vertex $\overline{v} \in \overline{V}$ corresponds to a face in the primal graph G and dual edges $\overline{e} \in \overline{E}$ correspond to the border separating the faces in the G [6, Section 4.6]. The gray value (g-value) of the pixel p is visually conceived as the height of the surface and it is denoted by $g(p) = g(v)$ where v is the corresponding vertex of p. There are two operations: contraction and removal defined on the edges of the graph. Contraction of edge [6, Section 1.7] in G will result in merging the two vertices connected by the respective edge. This is equivalent to the removal operation in $\overline{G}$. The removal of an edge $(v, w) \in E$ disconnects the two vertices v and w and merges the two faces which is equivalent to contract $\overline{e} \in \overline{E}$ in $\overline{G}$. There is a one-to-one correspondence between the edges of G and $\overline{G}$. By successively contracting and removing edges, we form a stack of progressively reducing planar graphs $(G_k, \overline{G_k}), k \in \{0, 1, \ldots, n\}$ where each graph G_{k+1} is smaller than the graph G_k [10, 1, 9]. The base level of the graph is the primal graph G_0.

Definition 1. *The **orientation of an edge** $(i, j) \in E$ in the primal graph $G = (V, E)$ is directed from vertex i to vertex j iff $g(i) > g(j)$.*

The edge $e \in E$ connecting two vertices $v, w \in V$ where $g(v) = g(w)$ are non-oriented. Note that we define orientation of edges by considering only the gray values as a feature of an image. The theory stated in this paper remains same for the higher dimensional feature vector if the orientation of edges is well defined for the domain.

The **LBP value** of an edge $e \in E$ connecting two vertices $v, w \in V$ is defined by comparing the g-values of the vertices. The LBP value of e is 1 if $g(v) > g(w)$ and it is 0 if $g(v) < g(w)$. The **LBP code** of vertex $v \in V$ is obtained by concatenating, in clockwise or counterclockwise orientation, the LBP value of edges incident to v (edges connecting vertices $v, w \in V$ such that $g(v) = g(w)$ are not considered when computing the LBP code of vertex v). LBP codes are used for the classification of vertices into maximum, minimum, saddle or slope point.

Definition 2. *A vertex v in graph G_k is a **local maximum** $\oplus$ if its LBP code consists of only 1s.*

Definition 3. *A vertex v in graph G_k is a **local minimum** $\ominus$ if its LBP code consists of only 0s.*

Definition 4. *A vertex v in graph G_k is a **slope point** if the circular permutation[1] of it's LBP code has exactly 2 bit switches.*

Definition 5. *A vertex v in graph G_k is a **saddle point** $\otimes$ if the circular permutation of it's LBP code has a number of bit switches greater than 2.*

[1] Circular permutation consists of rotating the code clockwise or counter-clockwise by 1 bit.

Fig. 1(a), (b), (c) and (d) are examples of a local maximum, a local minimum, a slope point and a saddle point respectively. The category of the vertex is decided by the orientation of the edges incident on the vertex and the categorization is independent of the number of the incident edges. Thus the theory can be generalized beyond the gray scale digital images, where the vertex may contain a vector of the values (for example: RGB), provided that the metric for the orientation of the edges is well defined.

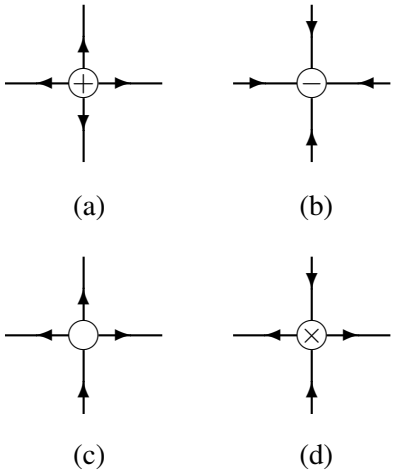

Figure 1. LBP categories and the orientation of the incident edges.

Definition 6. *A **path** π is a non empty sub-graph of G, consisting of an alternating sequence of vertices and edges $\pi = v_1, e(v_1, v_2), v_2, \ldots, e(v_{r-1}, v_r), v_r$. The LBP code of path π is obtained by consecutively concatenating the LBP value of edge $e(v_{i-1}, v_i)$ for $i \in \{2, 3, \ldots, r\}$. If there are no bit switches in the LBP code of π then π is a **monotonic path**. A monotonic path which contains at least one oriented edge is a **strictly monotonic path**.*

A **plateau** is a connected, non empty sub-graph $G_P = (V_P, E_P) \subset G = (V, E)$ such that every edge $(v, w) \in E_P$ of the plateau satisfies $g(v) = g(w)$. A **level curve** is a particular case of plateaus: It is a path along which all the vertices have the same g-value. Notice that a self-loop is also a level curve and edges of level curves are not oriented. Observe that a level curve can be a monotonic path but it cannot be a strictly monotonic path since a strictly monotonic path requires requires at least one oriented edge (i.e, an edge with LBP value). After performing the contraction of the edges of a plateau, the sub-graph is reduced to either a single vertex or a set of level curves incident to a common vertex.

A non-well composed configuration is modified to a well-composed configuration [14] by adding a dummy vertex which is a hidden saddle point [5]. Adding a hidden saddle includes addition of four edges incident on the hidden saddle point which ensures that no two local extrema of same category be part of the same face. It decomposes the respective face into four distinct slope regions with degree[2] three each.

The LBP codes are embedded after the contraction of all the edges in the plateau and adding the hidden saddles. The successive operations of contraction on edges may generate self-loops which are included in the model we provide in this document.

Definition 7. *A face in a surface embedded graph G is a **slope region** $\mathbb{S}$ if all the pairs of points in the surface corresponding to the face can be connected by a continuous monotonic curve inside the face.*

See the example of a slope region bounded by a level curve in Fig. 2d. The slope regions and their different configurations are discussed in [11, 12].

Remark 1. *The boundary $\delta\mathbb{S}$ of the slope region $\mathbb{S}$ can either be decomposed into exactly two monotonic paths or a level curve [11, Lemma 1].*

Remark 2. ***Properties of a slope region:** Saddle points can only exist on the boundary $\delta\mathbb{S}$ of the slope region $\mathbb{S}$ with additional edges incident to the saddle point outside the slope region. Saddle points cannot exist in the interior $\mathbb{S} \setminus \delta\mathbb{S}$ of the slope region $\mathbb{S}$ [11, Lemma 2].*

A well-composed sampled surface is a well-composed digital picture [13] which samples a continuous surface. The following property holds.

Lemma 1. *All the faces in the primal graph G_k after contraction of plateau regions in a well-composed sampled surface are slope regions.*

Proof. After collapsing the plateau region to a single vertex, the vertex is encoded by a LBP code which may result in a maximum, minimum, saddle or a slope point. If the plateau collapses into a level curve, a walk on level curves do not require an orientation of its edges. A contraction operation in the interior of graph will reduce the degree of the two face sharing the contracted edge. So after contracting the

[2]The degree of a face in primal graph is the number of edges surrounding the face.

plateau region, the maximum degree of a face in primal graph G_k will be four. After both the above mentioned operations (contraction of plateau and adding hidden saddles), the maximum degree of a face is four with a constraint that no two extrema of same category share the same face. In simple words, no two local maxima and no two local minima are on the same face. Thus we obtain an acyclic configuration of faces of degree 3 or 4 composed of not more than one maximum and one minimum. The remaining vertices are composed of slope points and / or saddles. The border of such face will always be composed of two distinct monotonic paths, i.e. the face is a slope region according to Remark 7. □

Lemma 2. *The minimum possible degree of a face to be a slope region is three.*

Proof. If the degree of a face is reduced to two, it simply means that the two vertices are connected by double edges and one of the edge can be removed to simplify the graph and eliminate redundant information. □

3. Minimal slope regions

In this section we enumerate the different possible configurations of slope regions which can be generated with a minimum number edges and the incident vertices are only critical points, also called *minimal slope regions*.

As mentioned in Lemma 2, the minimum number of oriented edges to form a slope region is three. Fig. 2 shows the possible configurations of minimal slope regions. Fig. 2a is a simple triangle which can be generated by categorizing the vertices A,B and C as maximum $\oplus$, minimum $\ominus$ and a saddle point $\otimes$ in random order. Fig. 2b is a non-simple triangle where vertex A can be a maximum or a minimum and has a self-loop encapsulated by the multiple edges connecting vertex A and B. This self-loop needs a further inside sub-graph S, otherwise it is redundant and removed by simplification. Fig. 2c is the reverse of Fig. 2b, where the face with multiple edges connecting vertices A and B is encapsulated by the self-loop attached to vertex A. Also in this case there must be a further sub-graph D between the double edges to avoid redundancy. Fig. 2d is the simplified version of Fig. 2c where one of the edge connecting vertices A and B is removed.

The motivation behind enumeration of minimal slope regions is to represent a sampled surface with slope regions formed by the critical points only. In this way, we can move ahead to our goal of counting the minimal number of slope regions (faces) in the primal graph G_k which also includes self-loops.

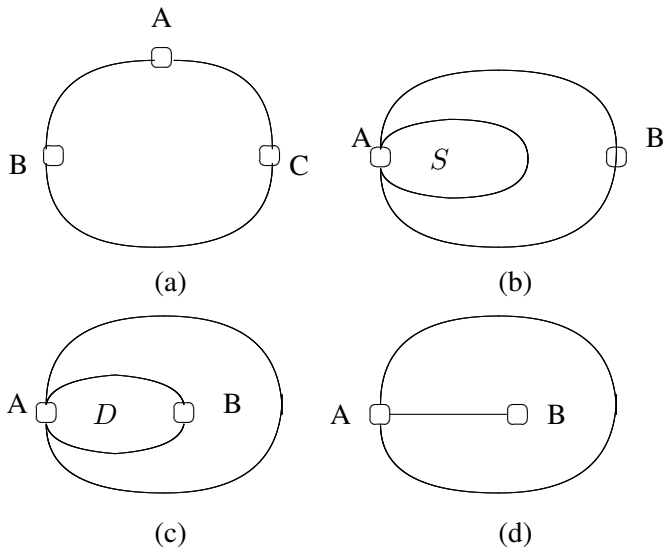

Figure 2. Configuration of slope regions with minimum number of vertices and edges.

4. Contraction of saddle components

Consider a graph G_k with all faces being minimal slope regions. The sub-graph formed by a connected component of saddle points can only have a tree structure [11, Remark 3]. In this section, we summarize the effect of contracting each saddle tree to a single point.

Lemma 3. *The number of faces of graph G_k remains the same after contracting all the connected saddle components of G_k.*

Proof. According to Lemma 1, all the faces in the primal graph G_k of a well-composed sampled surface are slope regions. The proof of Lemma 3 for a sub-graph of G_k composed of adjacent slope regions sharing saddle points can be extended to the whole graph G_k. Consider a sub-graph of G_k formed by a tree of saddle points and their incident edges and neighborhood vertices as shown in Figure 3a. Contraction of an edge in this saddle tree removes exactly one edge and one vertex. Substituting these values in Euler's formula, the number of faces will remain constant. It can be verified in Fig. 3b where the edges of the saddle tree are contracted into a single saddle point. The number of slope regions (faces) in G_k remains the same. □

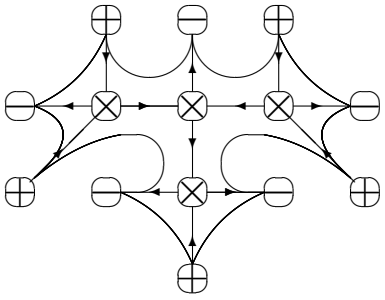

(a)

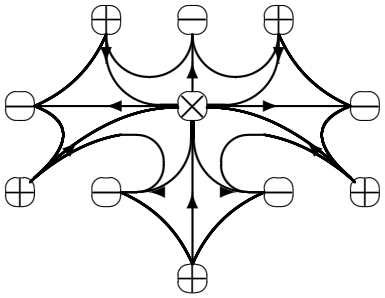

(b)

Figure 3. Sub-graph formed by a saddle tree before (a) and after (b) contraction

5. Combinations of slope regions

In this subsection we construct sub-graphs by combining different configurations of minimal slope regions mentioned in Section 3.

1. We start by generating a sub-graph formed by considering multiple occurrences of configuration Fig. 2a. We get a sub-graph with alternating sequence of maxima and minima surrounding a single saddle point as shown in Fig. 4

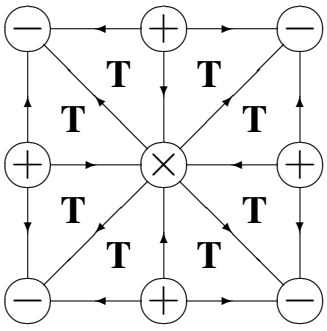

Figure 4. Saddle surrounded by 8 slope regions.

The slope region **T** in Fig. 4 is a simple triangle formed by critical points only. The lower limit of the number of slope regions **T** that can share the same saddle point is 2, while the upper limit is the total amount of slope regions on the surface.

2. The combination of self-loop and double edge configurations is more tricky. If we encapsulate configuration Fig. 2d inside Fig. 2b, we get a configuration of self-loop S_+ and S_- encapsulated by an alternating sequence of maxima and minima as shown in Fig. 5a, 5b respectively.

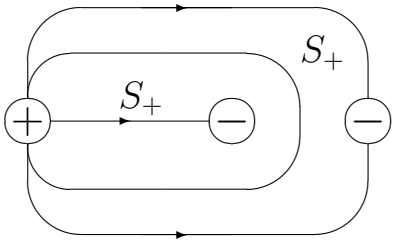

(a) Self-loop attached to $\oplus$.

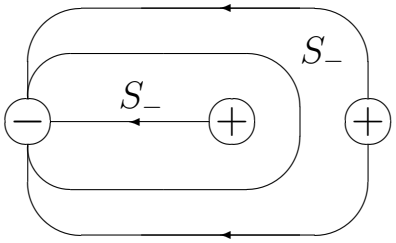

(b) Self-loop attached to $\ominus$.

Figure 5. Combining self-loops and double edges.

3. The self-loops attached to saddles show a simple $(S_{\times+}, S_{\times-})$ configuration (Fig. 6) and a more complex configuration involving the simple slope region **T**. The simple configurations can be combined similar to the self-loops at extrema:

   In this case, the orientation of $S_{\times+}$ and $S_{\times-}$ is opposite to each other to yield an outside double edge between the saddle and the extremum. The pending edge connected to the saddle outside the slope region must be complemented by the opposite extremum. It can be completed by a cycle around $\otimes$ similar to the simple triangles **T** above.

   The complex configurations $(S_{\times+}, \mathbf{T}, \mathbf{T})$ and $(S_{\times-}, \mathbf{T}, \mathbf{T})$ (Fig. 7) have on the outside a self-loop attached to the saddle. The self-loop of $S_{\times+}$ can be encapsulated into an $S_{\times-}$-configuration and the self-loop $S_{\times-}$ into an $S_{\times+}$- configuration. In both cases the outside is a double edge connecting two different extrema.

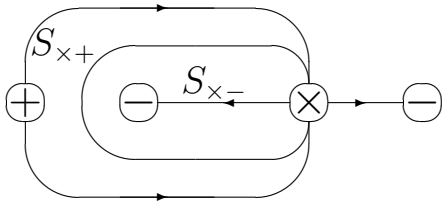

(a) $S_{\times-}$ inside $S_{\times+}$.

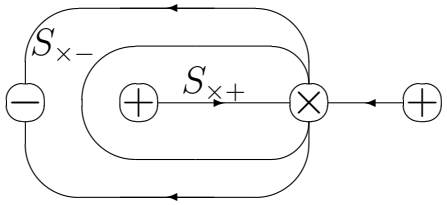

(b) $S_{\times+}$ inside $S_{\times-}$.

Figure 6. Combining self-loop and double edges attached to a saddle $\otimes$.

Hence it can be combined easily with any of the other configurations with alternating extrema on the outside.

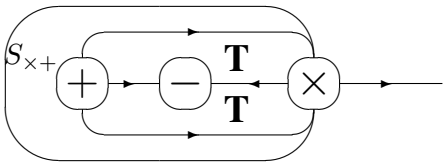

(a) $S_{\times+}$ encapsulating two slope regions **T** inside self loop.

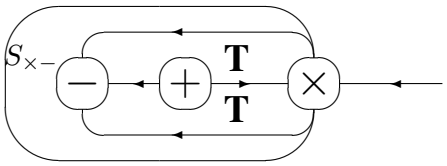

(b) $S_{\times-}$ encapsulating two slope regions **T** inside self loop.

Figure 7. Combining simple slope region **T** with self loop and double edges attached to $S_{\times+}$ and $S_{\times-}$

4. Alternatively, any of the configurations bounded by a double edge can be recursively embedded into a self-loop generating one more of the above primitive self-loop configurations. The completion towards the outside is then analogously as in the primitive configurations.

6. Number of slope regions

Let G_k be a graph composed of only critical points and with saddle trees being contracted. Then, the slope regions (faces of the graph) are separated by single edges only. Hence it makes sense to count the number of edges which serve as boundary between the two slope regions instead of counting the slope regions itself.

From now on, a $(\oplus,\ominus)$-edge of G_k is an edge connecting a maximum and a minimum. A $(\oplus,\ominus)$-bridge of G_k is a $(\oplus,\ominus)$-edge satisfying that its removal would disconnect the graph G_k.

Theorem 4. *Given a graph G_k made of critical points only with all the slope regions composed of maximum three edges, we apply following operations on G_k:*

1. *delete all $(\oplus,\ominus)$-edges inside the boundary of graph G_k,*
2. *keep all $(\oplus,\ominus)$-edges on the boundary of graph G_k,*
3. *keep all $(\oplus,\ominus)$-bridges, and*
4. *delete self-loops between $S_{\times+}, S_{\times-}$.*

The resulting graph is plane, all dual faces are slope regions and it cannot be further reduced without destroying the property that all faces are slope regions. The total number of slope regions corresponds to the sum of the following entities:

$$\begin{aligned}&|\{\text{ edge } (\oplus,\ominus) \text{ such that } \oplus \in V_\oplus \text{ and } \ominus \in V_\ominus\}|\\ &+|\{\text{ edge } (\otimes,\otimes) \text{ such that } \otimes \in V_\otimes \text{ and}\\ &\qquad\qquad \overline{(\otimes,\otimes)} = (S_{\times+}, S_{\times-})\}|.\end{aligned} \tag{1}$$

Remark that (1) counts for inner $(\oplus,\ominus)$-edges the merged slope regions but only one slope for outer $(\oplus,\ominus)$-edges and $(\oplus,\ominus)$-bridges. Multiple $(\oplus,\ominus)$-edges count only one slope.

Proof. Deletion of an edge does not change the planarity of a graph.

We show that the deletion of a $(\oplus,\ominus)$-edge or of the self-loop merges two slope regions into a new face which is a slope by considering the cases separately. A $(\oplus,\ominus)$-edge of G_k may be a $(\oplus,\ominus)$-bridge or it may be an inner $(\oplus,\ominus)$-edge of G_k. In the first two cases the $(\oplus,\ominus)$-edge bounds a single slope. Notice that a bridge need not be an outer edge and is therefore separately mentioned.

An inner $(\oplus,\ominus)$-edge in a triangular mesh is adjacent to two other triangles each being a slope with the same two local extrema. Hence the quadrilateral

formed after the removal of the $(\oplus, \ominus)$-edge is also a slope. The argument remains true after the first $(\oplus, \ominus)$-edge of multiple $(\oplus, \ominus)$-edges is removed. Therefore all multiple $(\oplus, \ominus)$-edges can be removed and the merged slope regions still share the same two extrema in a single slope.

The special configurations involving self-loops enumerated in Section 3 need to be considered with care: Self-loops attached to extrema inherit the property of being extremal from their anchor vertices. They separate inner and outer faces which are both either lower or higher than the self-loop. Every path connecting a point in the inner face with a point in the outer face must cross the self-loop which is extremal and, hence, the path cannot be monotonic.

However, self-loops attached to saddles surround either a higher slope $S_{\times+}$ or a lower slope $S_{\times-}$. $S_{\times+}$ can be embedded only inside $S_{\times-}$ and $S_{\times-}$ only inside $S_{\times+}$. In both cases the removal of the self-loop generates a face which contains one minimum and one maximum and is a valid slope.

Finally we proceed to show the given count of slope regions (1). We have shown in Lemma 3 that all edges attached to saddles do not have any influence on the number of slope regions. All edges between two saddles can be contracted without reducing the number of slope regions and saddles except self-loops cannot form cycles. The first part combines the first three cases while the count of self-loops attached to saddles follows the above arguments.

□

7. Conclusion

In this paper, we have formed a catalogue of different slope configuration which can be formed using critical points. We further enumerated all the possible combinations of slope regions which forms the basis to represent a surface. Then we provide a formula to count the number of slope regions in a graph of a surface. One possible extension of counting the number of slope regions is to serve as an objective quality measure of an algorithm of multi-resolution image segmentation.

References

[1] L. Brun and W. G. Kropatsch. Dual Contraction of Combinatorial Maps. In W. G. Kropatsch and J.-M. Jolion, editors, *2nd IAPR-TC-15 Workshop on Graph-based Representation*, pages 145–154. OCG-Schriftenreihe, Österreichische Computer Gesellschaft, 1999. Band 126. 2, 8

[2] P. J. Burt, T.-H. Hong, and A. Rosenfeld. Segmentation and estimation of image region properties through cooperative hierarchial computation. *IEEE Transactions on Systems, Man, and Cybernetics*, 11(12):802–809, 1981. 8

[3] A. Cayley. Xl. On contour and slope lines. *The London, Edinburgh, and Dublin Philosophical Magazine and Journal of Science*, 18(120):264–268, 1859. 1

[4] M. Cerman, R. Gonzalez-Diaz, and W. G. Kropatsch. LBP and Irregular Graph Pyramids. In N. Petkov and G. Azzopardi, editors, *Proceedings of the CAIP2015*, 2015. 1

[5] M. Cerman, I. Janusch, R. Gonzalez-Diaz, and W. G. Kropatsch. Topology-based image segmentation using LBP pyramids. *Machine Vision and Applications*, 27(8):1161–1174, 2016. 1, 3

[6] R. Diestel. Graph theory. 1997. *Grad. Texts in Math*, 1997. 2

[7] H. Edelsbrunner, J. Harer, V. Natarajan, and V. Pascucci. Morse-Smale complexes for piecewise linear 3-manifolds. In *Proceedings of the nineteenth annual symposium on Computational geometry*, pages 361–370. ACM, 2003. 1

[8] H. Edelsbrunner, J. Harer, and A. Zomorodian. Hierarchical Morse-Smale complexes for piecewise linear 2-manifolds. *Discrete and computational Geometry*, 30(1):87–107, 2003. 1

[9] Y. Haxhimusa and W. G. Kropatsch. Hierarchy of Partitions with Dual Graph Contraction. In E. Michaelis and G. Krell, editors, *DAGM 2003, 25th DAGM Symposium*, volume 2781 of *Lecture Notes in Computer Science*, pages 338–345, Magdeburg, Germany, September 2003. Springer, Berlin Heidelberg. 2

[10] W. G. Kropatsch. Building Irregular Pyramids by Dual Graph Contraction. *IEE-Proc. Vision, Image and Signal Processing*, Vol. 142(No. 6):pp. 366–374, December 1995. 2, 8

[11] W. G. Kropatsch, R. M. Casablanca, D. Batavia, and R. Gonzalez-Diaz. Computing and reducing slope complexes. In *Discrete Geometry for Com-puter Imagery*, volume 11382, pages 12–25. Springer, 2019. 1, 2, 3, 4

[12] W. G. Kropatsch, R. M. Casablanca, D. Batavia, and R. Gonzalez-Diaz. On the space between critical points. In *Computational Topology in Image Context - 7th International Workshop, CTIC 2019, Mlaga, Spain, January 24-25, 2019, Proceedings.* Springer, 2019. 1, 3

[13] L. Latecki, U. Eckhardt, and A. Rosenfeld. Well-composed sets. *Computer Vision and Image Understanding*, 61(1):70 – 83, 1995. 3

[14] L. J. Latecki. 3d well-composed pictures. *CVGIP: Graphical Model and Image Processing*, 59(3):164–172, 1997. 3

[15] R. N. Lee. Two-dimensional critical point configuration graphs. *IEEE Transactions on Pattern Analysis and Machine Intelligence*, 4:442–450, 1984. 1

[16] D. Martin, C. Fowlkes, D. Tal, and J. Malik. A database of human segmented natural images and its application to evaluating segmentation algorithms and measuring ecological statistics. In *Computer Vision, 2001. ICCV 2001. Proceedings. Eighth IEEE International Conference on*, volume 2, pages 416–423. IEEE, 2001. 8

[17] J. C. Maxwell. L. On hills and dales: To the editors of the philosophical magazine and journal. *The London, Edinburgh, and Dublin Philosophical Magazine and Journal of Science*, 40(269):421–427, 1870. 1

[18] A. Montanvert, P. Meer, and A. Rosenfeld. Hierarchical image analysis using irregular tessellations. *IEEE Transactions on Pattern Analysis & Machine Intelligence*, 4:307–316, 1991. 8

[19] X. Wei, Q. Yang, Y. Gong, N. Ahuja, and M.-H. Yang. Superpixel hierarchy. *IEEE Transactions on Image Processing*, 27(10):4838–4849, 2018. 1

8. Appendix

In this section, we show examples of multi-resolution image segmentation using combinatorial graph pyramid. Due to lack of flexibility in the regular pyramid [2], irregular pyramids [18] were introduced. Irregular pyramids can be stored in various data structures like adjacency graphs, dual graphs, combinatorial maps, etc. We use a stack of combinatorial maps to form combinatorial pyramids [10, 1]. Similar to graphs, we define the operation of contraction and removal of edges in the combinatorial pyramid. Edges are removed or contracted in the primal graph as long as the resulting faces continue to be slope regions. Formation of graph pyramid may result in generation of the self-loops and multiple edges between the vertices. Hence it becomes important to count the number of slope regions in primal graph (dual vertices) which essentially are the number of segments at the given level of the graph pyramid, which was the main task of this paper.

We used the Berkeley Image Segmentation Dataset [16] which consists of images of size $481 \times 321 = 154401$ pixels. That means, at the base level of the graph pyramid, there are 154401 vertices and 153600 faces. The results below show the original image and the processed image with more than 90% reduction of slope regions. It can be clearly observed in Fig. 8 and Fig. 9, that the texture information in the image is preserved and the contour effect can be seen on the region with smooth gradient.

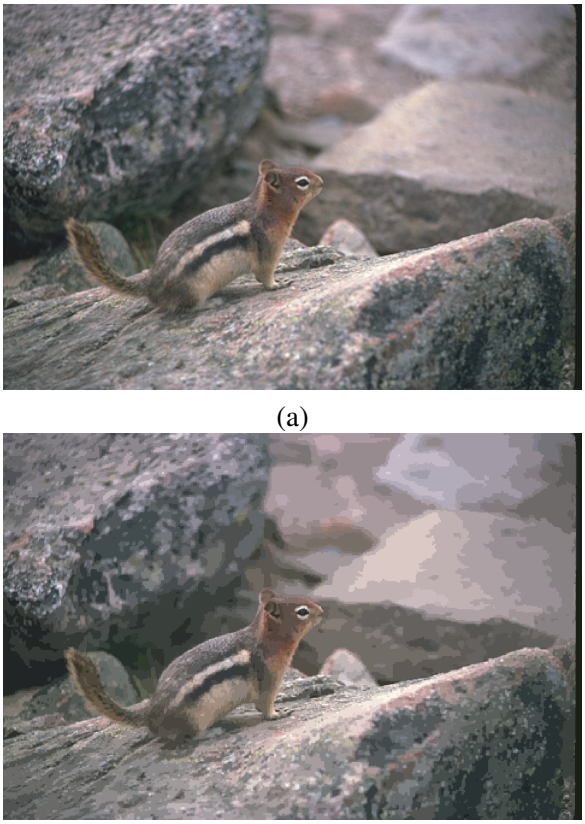

(a)

(b)

Figure 8. (a) Original image of size 481×321 with 154401 regions and (b) has 9264 regions i.e. 94% reduction.

(a)

(b)

Figure 9. (a) Original image of size 481×321 with 154401 regions and (b) has 15440 regions i.e. 90% reduction.